Chapter 5

FE-MEDIATED NITROGEN FIXATION WITH A METALLOCENE MEDIATOR: EXPLORING P*K*A EFFECTS AND DEMONSTRATING ELECTROCATALYSIS

Reproduced in part with permission from:

Chalkley, M.; Del Castillo, T.; Matson, B.; Peters, J. C.; *J. Am. Chem. Soc.*, **2018**, accepted.

DOI: 10.1021/jacs.8b02335

We've reached the final chapter of our tale. I'm afraid I don't have a particular message to accompany this project, perhaps it is still too fresh for me to have formed an impression of it. I'll relate here that, as I've alluded to, demonstrating electrocatalytic N_2RR was one of the very first targets I latched onto when I started my research with Jonas. The idea seemed optimistic (to say the least) at the time and even until almost the end of my fifth year I didn't think I would see this result in my time at Caltech. I suppose something can be said here for persistence in pursuing a goal, but probably the better message is that while it is important to work towards big, overarching targets it is also important to be open to things you discover along the way.

5.1 Introduction

There has been substantial recent progress in the development of soluble, well-defined molecular catalysts for N_2-to-NH_3 conversion, commonly referred to as the nitrogen reduction reaction (N_2RR).[1] Nevertheless, a significant and unmet challenge is to develop molecular catalysts, and conditions, compatible with electrocatalytic N_2RR. Progress in this area could have both fundamental and practical benefits, including access to informative in situ mechanistic studies via electrochemical techniques, and an electrochemical means to translate solar or otherwise derived chemical currency (H^+/e^-) into NH_3. The latter goal, which has been the subject of numerous studies using heterogeneous catalysts, is key to the long-term delivery of new ammonia synthesis technologies for fertilizer and/or fuel.[2]

Many soluble coordination complexes are now known that electrocatalytically mediate the hydrogen evolution reaction (HER),[3] the carbon dioxide reduction reaction (CO_2RR),[4] and the oxygen reduction reaction (O_2RR).[5] The study of such systems has matured at a rapid pace in recent years, coinciding with expanded research efforts towards solar-derived fuel systems. In this context, it is noteworthy how little corresponding progress has been made towards the discovery of soluble molecular catalysts that mediate electrocatalytic N_2RR. To our knowledge, only two prior systems address this topic directly.[6,7,8]

More than three decades ago, Pickett and coworkers reported that a Chatt-type tungsten-hydrazido(2−) complex could be electrochemically reduced to release ammonia (and trace hydrazine), along with some amount of a reduced tungsten-dinitrogen product; the latter species serves as the source of the tungsten-hydrazido(2−) complex (via its protonation by acid).[6a] By cycling through such a process, an electrochemical, but not an electrocatalytic, synthesis of ammonia was demonstrated. Indeed, efforts to demonstrate electrocatalysis with this and related systems instead led to substoichiometric NH_3 yields.[6c]

An obvious limitation to progress in electrochemical N_2RR by molecular systems concerns the small number of synthetic N_2RR catalysts that have been available for study; it is only in the past five years that sufficiently robust catalyst systems have been identified to motivate such studies. In addition, the conditions that have to date been employed to mediate N_2RR have typically included non-polar solvents, such as heptane, toluene, and diethyl ether (Et_2O), that are not particularly well-suited to electrochemical studies owing to the lack of compatible electrolytes.[1]

Nevertheless, several recent developments, including ones from our lab, point to the likelihood that iron (and perhaps other) molecular coordination complexes may be able to mediate electrocatalytic N_2RR in organic solvent. Specifically, our lab recently reported that a tris(phosphine)borane iron complex, $P_3^BFe^+$, that is competent for catalytic N_2RR with chemical reductants, can also mediate electrolytic N_2-to-NH_3 conversion,[6d] with the available data (including that presented in this study) pointing to bona fide electrocatalysis in Et_2O.

Focusing on the $P_3^BFe^+$ catalytic N_2RR system, a development germane to the present study was its recently discovered compatibility with reagents milder than those that had been originally employed.[1c] Thus, decamethylcobaltocene (Cp^*_2Co) and diphenylammonium acid are effective for N_2RR catalysis; these reagents give rise to fast, and also quite selective (> 70% vs HER), N_2RR catalysis at low temperature and pressure in ethereal solvent. In addition, based on preliminary spectroscopic evidence and density functional theory (DFT) predictions, it appears that a protonated metallocene species, $Cp^*(\eta^4\text{-}C_5Me_5H)Co^+$, may be an important intermediate of N_2RR catalysis under such conditions. Indeed, we have suggested that $Cp^*(\eta^4\text{-}C_5Me_5H)Co^+$ may serve as a proton-coupled-electron-transfer (PCET) donor ($BDE_{C–H}$(calc) = 31 kcal mol^{-1}), thereby mediating net H-atom transfers to generate N–H bonds during N_2RR.[9] The presence of a metallocene mediator might, we therefore reasoned, enhance N_2RR during electrocatalysis.

We present here a study of the effect of pK_a on the selectivity of $P_3^BFe^+$ for N_2RR vs HER. By using substituted anilinium acids, we are able to vary the acid pK_a over 9 orders of magnitude and find that the selectivity is highly correlated with the pK_a. In our efforts to investigate the origin of the observed pK_a effect, we found, to our surprise, that in stoichiometric reactions, the catalytically competent anilinium triflate acids are unable to faciltate productive N–H bond formation with early-stage N_2-fixation intermediates. We therefore hypothesize that the formation of a protonated metallocene species, $Cp^*(\eta^4\text{-}C_5Me_5H)Co^+$, plays a critical role in N–H bond-forming reactions, either via PCET, PT, or a combination of both during N_2RR catalysis. DFT studies support this hypothesis and also establish that the observed pK_a correlation with N_2RR selectivity can be explained by the varying ability of the acids to protonate Cp^*_2Co. The suggested role of this protonated metallocene intermediate in N–H bond forming reactions led us to test the effect of $Cp^*_2Co^+$ as an additive in the electrolytic synthesis of NH_3 mediated by $P_3^BFe^+$. We find that the addition of co-catalytic $Cp^*_2Co^+$ enhances the yield of NH_3 without decreasing the Faradaic efficiency (FE), and furnishes what is to our knowledge the first unambiguous demonstration of electrocatalytic N_2RR mediated by a soluble, molecular coordination complex.

5.2 Results and Discussion

5.2.1 pK_a Studies.

In our recent study on the ability of $P_3^BFe^+$ to perform N_2RR with $Cp^*{}_2Co$ as the chemical reductant,[9] we found that there was a marked difference in efficiency for NH_3 generation with diphenylammonium triflate ($[Ph_2NH_2][OTf]$) versus anilinium triflate ($[PhNH_3][OTf]$). In that study, we posited that this difference could arise from several possibilities, including the differential solubility, sterics, or pK_a's of these acids.[9]

To investigate the last possibility, we have studied the efficiency of the catalysis by quantifying the NH_3 and H_2 produced when using substituted anilinium acids with different pK_a values (Table 5.1). The table is organized in increasing acid strength, from $[^{4\text{-}OMe}PhNH_3][OTf]$ as the weakest acid to the perchlorinated derivative ($[^{per\text{-}Cl}PhNH_3][OTf]$) as the strongest. Importantly, good total electron yields (85.8 ± 3.3) were obtained in all cases. As can be seen from the table, the NH_3 efficiencies are found to be strongly correlated with pK_a.[10]

In particular, a comparison of the efficiency for NH_3 with the pK_a of the anilinium acid used gives rise to four distinct activity regimes (Table 5.1, Figure 5.1). One regime that is completely inactive for N_2RR, but active for HER, is defined by the weakest acid, $[^{4\text{-}OMe}PhNH_3][OTf]$ (pK_a = 8.8).[11] A gradual increase in observed NH_3 yields, coupled with a decrease in H_2 yield, comprises a second regime, in which the acid is strengthened from $[PhNH_3][OTf]$ (pK_a = 7.8), to $[^{2,6\text{-}Me}PhNH_3][OTf]$ (pK_a = 6.8), to $[^{2\text{-}Cl}PhNH_3][OTf]$ (pK_a = 5.6). Yet stronger acids, $[^{2,5\text{-}Cl}PhNH_3][OTf]$ (pK_a = 4.3), $[^{2,6\text{-}Cl}PhNH_3][OTf]$ (pK_a = 3.4), and $[^{2,4,6\text{-}Cl}PhNH_3][OTf]$ (pK_a = 2.1), constitute another, most active N_2RR regime, one in which the H_2 yields are nearly invariant.[12] The highest selectivity for N_2RR (~ 78%) was observed using [$^{2,5\text{-Cl}}$PhNH$_3$][OTf] as the acid. A final regime of very low N$_2$RR activity is encountered with [$^{\text{per-Cl}}$PhNH$_3$][OTf] (pK_a = 1.3) as the acid. We suspect this last acid undergoes unproductive

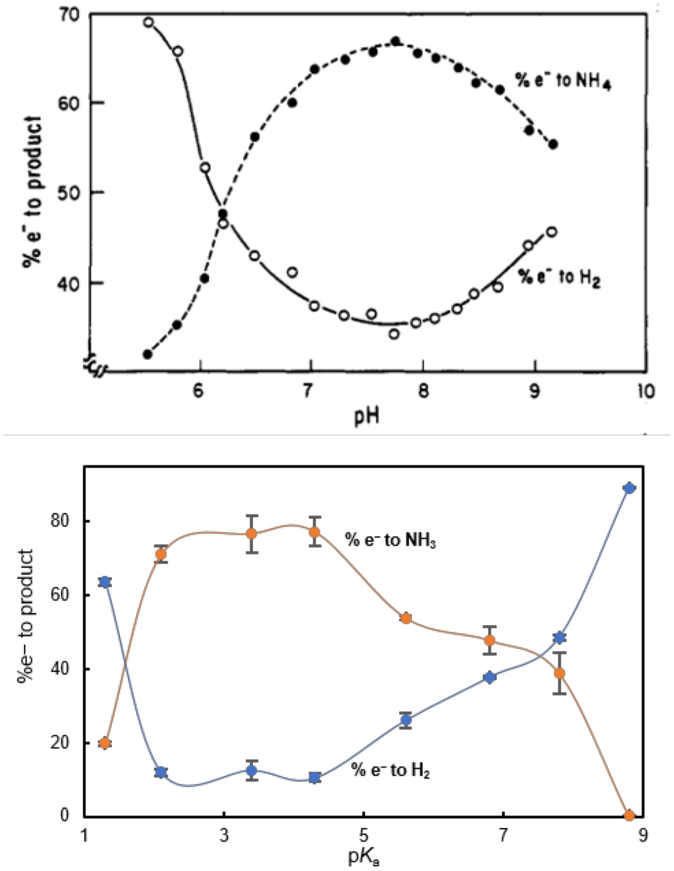

Figure 5.1. (top) Percentage of electrons being used to form NH$_3$ or H$_2$ at different pH values by the FeMo-nitrogenase in *A. vinelandii*. Reprinted with permission from Pham, D. N.; Burgess, B. K. *Biochemistry* **1993**, *32*, 13725. Copyright 1993 American Chemical Society. (bottom) Percentage of electrons being used to form NH$_3$ or H$_2$ at different pK_a values by P$_3$^{B}Fe$^+$.

Table 5.1. Literature and calculated pK_a values and efficiencies observed in catalytic N_2-to-NH_3 conversion

	pK_a^{exp} (THF)[10]	pK_a^{calc} (298 K)[a]	pK_d^{calc} (195 K)[b]	Equiv of NH_3/Fe	% yield of NH_3/e^-	% yield of H_2/e^-[c]
$[^{4\text{-OMe}}\text{PhNH}_3][\text{OTf}]$	8.8	9.6	15.7	0.04 ± 0.01	0.2 ± 0.1	89.1 ± 0.2
$[\text{PhNH}_3][\text{OTf}]$	7.8	7.7	13.8	7.3 ± 0.1	40.4 ± 0.5	48.6 ± 0.7
$[^{2,6\text{-Me}}\text{PhNH}_3][\text{OTf}]$	6.8	7.3	13.2	8.6 ± 0.7	47.5 ± 4.0	37.8 ± 0.2
$[\text{Cp}^*(exo\text{-}\eta^4\text{-}\text{C}_5\text{Me}_5\text{H})\text{Co}][\text{OTf}]$	N/A	9.2	11.8	—	—	—
$[^{2\text{-Cl}}\text{PhNH}_3][\text{OTf}]$	5.6	5.6	6.0	10.7 ± 0.1	53.9 ± 0.4	26.1 ± 1.9
$[^{2,5\text{-Cl}}\text{PhNH}_3][\text{OTf}]$	4.3	4.0	5.0	13.9 ± 0.7	77.5 ± 3.8	10.5 ± 1.1
$[^{2,6\text{-Cl}}\text{PhNH}_3][\text{OTf}]$	3.4	3.4	3.4	13.8 ± 0 .9	76.7 ± 4.9	12.6 ± 2.5
$[^{2,4,6\text{-cl}}\text{PhNH}_3][\text{OTf}]$	2.1	2.7	1.8	12.8 ± 0.4	70.9 ± 2.2	12.0 ± 0.8
$[^{\text{per-Cl}}\text{PhNH}_3][\text{OTf}]$	1.3	0.8	0.4	3.6 ± 0.1	19.9 ± 0.5	63.5 ± 1.1

$[^{4\text{-OMe}}\text{PhNH}_3][\text{OTf}]$ = 4-methoxyanilinium triflate, $[\text{PhNH}_3][\text{OTf}]$ = anilinium triflate, $[^{2,6\text{-Me}}\text{PhNH}_3][\text{OTf}]$ = 2,6-dimethylanilinium triflate, $[^{2\text{-Cl}}\text{PhNH}_3][\text{OTf}]$ = 2-chloroanilinium triflate, $[^{2,5\text{-Cl}}\text{PhNH}_3][\text{OTf}]$ = 2,5-dichloroanilinium triflate, $[^{2,6\text{-Cl}}\text{PhNH}_3][\text{OTf}]$ = 2,6-dichloroanilinium triflate, $[^{2,4,6\text{-Cl}}\text{PhNH}_3][\text{OTf}]$ = 2,4,6-trichloroanilinium triflate, $[^{\text{per-Cl}}\text{PhNH}_3][\text{OTf}]$ = 2,3,4,5,6-pentachloroanilinium triflate. [a]Acidities calculated at 298 K in THF and referenced to the known literature value for $[^{2,6\text{-Cl}}\text{PhNH}_3][\text{OTf}]$. [b] All species calculated as the ion-paired OTf^- species in Et_2O at 195 K and referenced to the known literature value for $[^{2,6\text{-Cl}}\text{PhNH}_3][\text{OTf}]$ in THF.

reduction via ET, thereby short-circuiting N_2RR. The only other N_2RR system for which this type of acid-dependent correlation has been systematically studied is the enzyme MoFe-nitrogenase.[13,14] As shown in Figure 5.1, the N_2RR vs HER activity of $P_3^BFe^+$ as a function of acid strength, is, in broad terms, similar to the behavior of the enzyme[13] across a wide pH range.

In a previous study of $Cp*_2Co$-mediated N_2RR by $P_3^BFe^+$,[9] we identified that $P_3^BFeN_2^-$ forms under the catalytic conditions. Earlier studies on the reactivity of $P_3^BFeN_2^-$ with an excess of soluble acids, including HOTf and $[H(OEt_2)_2][BAr^F_4]$ ($HBAr^F_4$, BAr^F_4 = tetrakis(3,5- bis(trifluoromethyl)phenyl)borate)), at −78 °C in Et_2O, established rapid formation of the doubly protonated species, $P_3^BFeNNH_2^+$.[15] Recent computational work from our group suggests that, under catalytic conditions with a soluble acid, different efficiencies for N_2RR (versus HER) by P_3^EFe catalysts (E = B, C, Si) are likely correlated to the rate of formation and consumption of early N_2RR intermediates (i.e., P_3^EFeNNH and $P_3^EFeNNH_2^{+/0}$).[16] Thus, we were interested in the reactivity of these anilinium triflate acids with $P_3^BFeN_2^-$, reasoning they may show differential efficiency in the formation of $P_3^BFeNNH_2^+$.

To our surprise, a freeze-quench EPR spectrum of the reaction of excess $[^{2,6\text{-}Cl}PhNH_3][OTf]$ (high N_2RR efficiency regime) at −78 °C in Et_2O with $P_3^BFeN_2^-$ does not show any $P_3^BFeNNH_2^+$. Also, freeze-quench Mössbauer analysis shows the formation of the oxidized products $P_3^BFeN_2$ and $P_3^BFe^+$, but nothing assignable to $P_3^BFeNNH_2^+$ (see SI for relevant spectra). Analysis of such a reaction for NH_3 or N_2H_4 after warming shows no fixed-N products. The observation of exclusive oxidation, rather than productive N–H bond formation, is analogous to what is observed upon addition of 1 equiv of a soluble acid

($HBAr^F_4$ or HOTf) to $P_3^BFeN_2^-$. We have previously suggested that if unstable P_3^BFeNNH is formed (eq 1) without excess acid to trap it (to form more stable $P_3^BFeNNH_2^+$, eq 2), then it can decay bimolecularly with the loss of 1/2 H_2 to form $P_3^BFeN_2$ (eq 3).

$$P_3^BFeN_2^- + H^+ \rightarrow P_3^BFeNNH \tag{1}$$

$$P_3^BFeNNH + H^+ \rightarrow P_3^BFeNNH_2^+ \tag{2}$$

$$P_3^BFeNNH \rightarrow P_3^BFeN_2 + 1/2\ H_2 \tag{3}$$

The low solubility of the anilinium triflate acids studied herein, in excess (50 equiv) and under the catalytically relevant conditions (1 mL Et_2O, −78 °C), likely leads to a similar scenario; consequently, P_3^BFeNNH that is generated is not efficiently captured by excess acid, leading instead to bimolecular H_2 loss. In accord with this idea, a freeze-quench EPR spectrum of the addition of 50 equiv of [$^{2,6\text{-}Cl}PhNH_3$][BAr^F_4], a far more ether soluble derivative of the same anilinium, to $P_3^BFeN_2^-$ shows $P_3^BFeNNH_2^+$ formation, and the detection of fixed-N products upon warming (0.20 ± 0.04 eq. NH_3 per Fe).

These observations must next be reconciled with the seemingly contradictory observation that comparatively efficient N_2RR catalysis is observed when [$^{2,6\text{-}Cl}PhNH_3$][OTf], and other anilinium triflate acids, are employed under catalytic conditions. For example, [Ph_2NH_2][OTf] leads to better efficiency for NH_3 formation versus [Ph_2NH_2][BAr^F_4] (72 ± 3% and 42 ± 6%, respectively). A key difference between the stoichiometric reactions described above, and the catalytic reaction, is the presence of Cp^*_2Co in the latter.

We have suggested that Cp^*_2Co can be protonated under the catalytic reaction conditions, to form $Cp^*(\eta^4\text{-}C_5Me_5H)Co^+$,[9] which may then play a role in N–H bond forming steps.[17] The results presented here (and below) suggest that such a mechanism is not only plausible, but is likely necessary, to explain the observed catalytic results with anilinium triflate acids. Given the effect of pK_a on the efficiency for N_2RR, we now hypothesize that this effect can arise from the relative energetics and rates of Cp^*_2Co protonation by the different anilinium triflate acids.

5.2.2 Computational Studies.

To investigate the kinetics and thermodynamics of Cp^*_2Co protonation by anilinium triflate acids we turned to a computational study. DFT-D3[18] calculations were undertaken at the TPSS/def2-TZVP(Fe); def2-SVP[19] level of theory, as used previously for studies of this $P_3^BFe^+$ system.[20] The free energy of H^+ exchange (ΔG_a) was calculated for all of the anilinium acids used (representative example shown in eq 4), and also for Cp*(*exo*-η^4-C_5Me_5H)Co^+, in Et_2O at 298 K. These free energies were then used to determine the acid pK_a's, with inclusion of a term to reference them to the literature pK_a value for [$^{2,6\text{-}Cl}PhNH_3$][OTf] at 298 K in THF (eq 5).

$$PhNH_2 + {}^{2,6\text{-}Cl}PhNH_3^+ \rightarrow PhNH_3^+ + {}^{2,6\text{-}Cl}PhNH_2 \quad (4)$$

$$pK_a(PhNH_3^+) = -\Delta G_a/(2.303\times RT) + pK_a({}^{2,6\text{-}Cl}PhNH_3^+) \quad (5)$$

Because we presume that variable triflate hydrogen bonding effects (0.5-10 kcal mol^{-1}) are likely to be important under the catalytic conditions (low temperature and low polarity solvent), we additionally calculated the free energy for net HOTf exchange reactions (ΔG_d) at 195 K in Et_2O (representative example shown in eq 6). The free energies of these reactions can then be used to determine a pK_d, referenced to the pK_a value for [$^{2,6\text{-}Cl}PhNH_3$][OTf] at 298 K in THF, for ease of comparison (eq 7). Hereafter, we use these pK_d values for discussion, but note that use of the pK_a values instead does not substantively alter the conclusions drawn.

$$PhNH_2 + [^{2,6\text{-}Cl}PhNH_3][OTf] \rightarrow$$

$$[PhNH_3][OTf] + {}^{2,6\text{-}Cl}PhNH_2 \quad (6)$$

$$pK_d([PhNH_3][OTf]) = -\Delta G_d/(2.303\times RT) + pK_a(^{2,6\text{-}Cl}PhNH_3^+) \quad (7)$$

Calculations of the pK_d of all of the relevant species (Table 5.1) shows that the pK_d of $[Cp^*(\textit{exo}\text{-}\eta^4\text{-}C_5Me_5H)Co][OTf]$ ($pK_d^{calc} = 11.8$; Table 5.1) falls within the range of the anilinium acids studied ($0.4 \leq pK_d^{calc} \leq 15.7$), suggesting there should be a significant acid dependence on the kinetics and thermodynamics of Cp^*_2Co protonation. To better elucidate the differences in Cp^*_2Co protonation between the acids studied, we investigated the kinetics of protonation for three acids, $[^{2,6\text{-}Cl}PhNH_3][OTf]$ (high selectivity; $pK_d^{calc} = 3.4$), $[^{2,6\text{-}Me}PhNH_3][OTf]$ (modest selectivity; $pK_d^{calc} = 13.2$), and $[^{4\text{-}OMe}PhNH_3][OTf]$ (poor selectivity; $pK_d^{calc} = 15.8$).

Transition states for Cp^*_2Co protonation were located for all three acids. To confirm that these transition states accurately reflect proton transfer, internal reaction coordinates (IRC) were followed to determine the reactant (IRC-A) and product (IRC-B) minima (Figure 5.2). These minima represent hydrogen bonded arrangements of the reactants and products. Protonation is found to have only a moderate barrier ($\Delta G^\ddagger$ in kcal mol^{-1}) in all three cases: ($[^{4\text{-}OMe}PhNH_3][OTf]$, +4.5; $[^{2,6\text{-}Me}PhNH_3][OTf]$, +3.8; $[^{2,6\text{-}Cl}PhNH_3][OTf]$, +1.3).

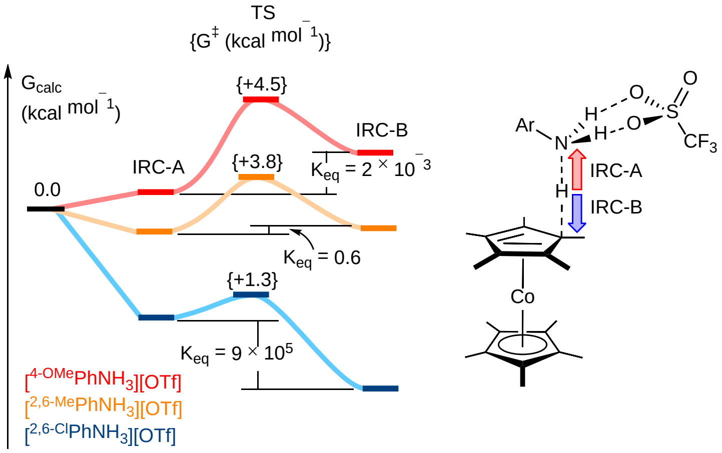

Figure 5.2. The kinetics and thermodynamics of protonation of Cp^*_2Co for three acids from different catalytic efficiency regimes ($[^{4\text{-OMe}}PhNH_3][OTf]$ = poor selectivity]; $[^{2,6\text{-Me}}PhNH_3][OTf]$ = modest selectivity; $[^{2,6\text{-Cl}}PhNH_3][OTf]$ = high selectivity).

This suggests that Cp^*_2Co protonation is kinetically accessible in all cases, in agreement with the experimental observation of background HER with each of these acids (see SI).

The small differences in rate, and the large variance in the equilibrium constant K_{eq} defined in eq 8, points to a significant difference in the population of protonated metallocene, $[Cp^*(exo\text{-}\eta^4\text{-}C_5Me_5H)Co][OTf]$, for these anilinium acids during catalysis.

$$K_{eq} = \frac{[^{R}PhNH_2{-}Cp^*(exo{-}\eta^4{-}C_5Me_5H)Co^+]}{[^{R}PhNH_3^+{-}Cp^*_2Co]} \qquad (8)$$

We reason that the low solubility of the anilinium triflate acids, and the low catalyst concentration (2.3 mM P_3^BFe), leads to a scenario in which the interaction between the acid and the Cp^*_2Co, the latter being present in excess relative to the iron catalyst (measured solubility of Cp^*_2Co at −78 °C in Et_2O is ~ 6 mM, see SI), significantly affects the overall kinetics of productive N–H bond formation. As such, the difference in $[Cp^*(exo\text{-}\eta^4\text{-}C_5Me_5H)Co][OTf]$ concentration and formation rate should relate to, and likely dominate, the origin of the observed pK_a effect. This explanation, rather than one that involves differences in rates for the direct interaction of a given $P_3^BFeN_xH_y$ species with an anilinium acid, better captures the collected data available.[21]

[Cp*(*exo*-η^4-C_5Me_5H)Co][OTf], characterized by a very weak C–H bond, should be a strong PCET donor, and we presume it serves such a role under the catalytic conditions being discussed herein.[22] Its reactions with $P_3^BFeN_xH_y$ intermediates may occur in a synchronous fashion, akin to HAT, or in an asynchronous fashion more akin to a PT-ET reaction.[23] While many $P_3^BFeN_xH_y$ intermediates may, at least in part, be generated via PCET with [Cp*(*exo*-η^4-C_5Me_5H)Co][OTf],[24] available experimental data point to a critical role for such a reaction via trapping of the highly reactive first fixed intermediate, P_3^BFeNNH (**Figure 5.3**), before it can bimolecularly release H_2 (eq 3). We hence investigated this reaction in more detail.

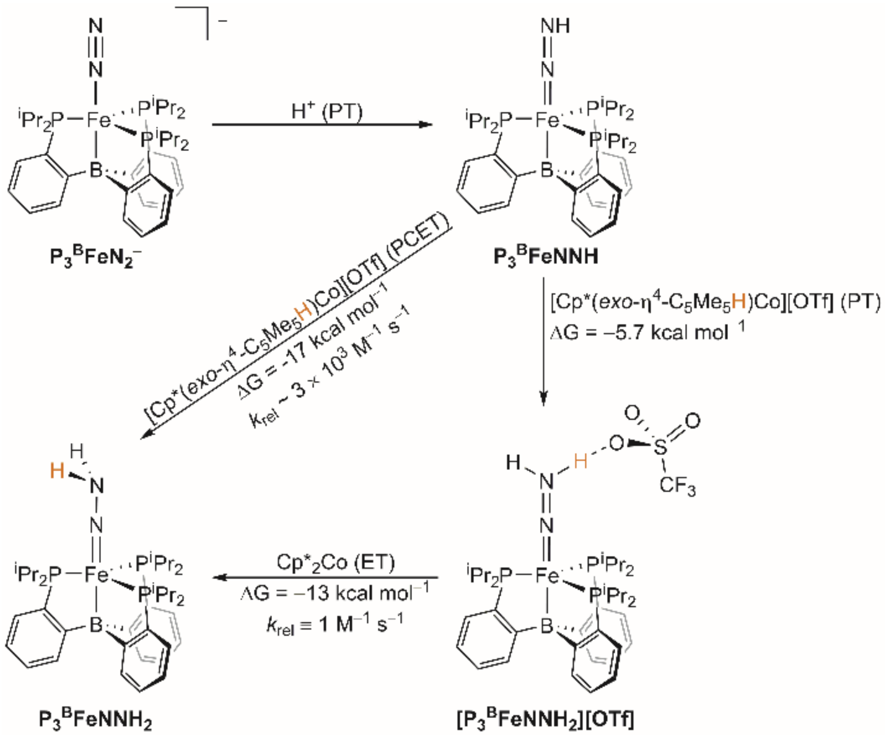

Figure 5.3. The calculated thermodynamics and kinetics of synchronous PCET and asynchronous PCET (PT-ET), between P_3^BFeNNH and $[Cp^*(exo\text{-}\eta^4\text{-}C_5Me_5H)Co][OTf]$ to generate $P_3^BFeNNH_2$. Note: k_{rel} for ET is defined as $1\ M^{-1}\ s^{-1}$.

Both a synchronous PCET ($\Delta G_{PCET} = -17.3$ kcal mol^{-1}; eq 9) and an asynchronous PCET path ($\Delta G_{PT} = -5.7$ kcal mol^{-1}, $\Delta G_{ET} = -11.6$ kcal mol^{-1}; eq 10 and 11), are predicted to be thermodynamically favorable.

$$P_3^BFeNNH + [Cp^*(exo\text{-}\eta^4\text{-}C_5Me_5H)Co][OTf] \rightarrow$$

$$P_3^BFeNNH_2 + [Cp^*_2Co][OTf] \qquad (9)$$

$$P_3^BFeNNH + [Cp^*(exo\text{-}\eta^4\text{-}C_5Me_5H)Co][OTf] \rightarrow$$

$$[P_3^BFeNNH_2][OTf] + Cp^*_2Co \qquad (10)$$

$$[P_3^BFeNNH_2][OTf] + Cp^*_2Co \rightarrow$$

$$P_3^BFeNNH_2 + [Cp^*_2Co][OTf] \qquad (11)$$

To evaluate the kinetics of these reactions the Marcus theory expressions[25] and the Hammes-Schiffer method[26] were used to approximate relative rates of bimolecular ET and PCET. We find that there is a slight kinetic preference for the fully synchronous PCET reaction ($k_{\mathrm{rel}}^{\mathrm{PCET}}$ ~ 3×10^3 $\mathrm{M^{-1}s^{-1}}$) compared to the fully asynchronous PT-ET reaction ($k_{\mathrm{rel}}^{\mathrm{PT\text{-}ET}} \approx k_{\mathrm{rel}}^{\mathrm{ET}} \equiv 1$ $\mathrm{M^{-1}\,s^{-1}}$; Figure 5.3).[27]

The above discussion leads to the conclusion that the efficiency for NH_3 formation in this system is coupled to the kinetics and/or thermodynamics of the reaction between the anilinium triflate acid and the $Cp^*{}_2Co$ reductant. This conclusion is counterintuitive, as the protonation of $Cp^*{}_2Co$ is also the requisite first step for background HER.[28] The fact that a key HER intermediate can be intercepted and used for productive N_2RR steps is an important design principle for such catalysis. Similar design strategies are currently being used to repurpose molecular cobalt HER catalysts for the reduction of unsaturated substrates.[29]

Efforts are often undertaken to suppress background reactivity between acid and reductant in catalytic N_2RR systems.[1a-b] We were hence particularly interested to explore whether the inclusion of a metallocene co-catalyst, in this case $Cp^*{}_2Co$, might improve the yield, and/or the Faradaic efficiency (FE), for N_2RR versus HER, in controlled potential electrolysis (CPE) experiments with $P_3^BFe^+$ under N_2.

5.2.3 Electrolysis Studies.

To set the context for this section of the present study, we had shown previously that ~ 2.2 equiv NH_3 (per Fe) could be generated via controlled potential electrolysis (CPE; −2.3 V vs $Fc^{+/0}$) at a reticulated vitreous carbon working electrode, using $P_3^BFe^+$ as the (pre)catalyst in the presence of $HBAr^F{}_4$ (50 equiv) at −45 °C under an atmosphere of N_2.

This yield of NH_3 corresponded to a ~ 25% FE which, while modest in terms of overall chemoselectivity, compares very favorably to FE's most typically reported for heterogeneous electrocatalysts for N_2RR that operate below 100 °C (< 2%).[2,30]

To further explore the possibility of using $P_3^BFe^+$ as an electrocatalyst for N_2RR, various conditions were surveyed to determine whether enhanced yields of NH_3 could be obtained from CPE experiments. For example, various applied potentials were studied (ranging from −2.1 to −3.0 V vs $Fc^{+/0}$), the concentrations of $P_3^BFe^+$ and $HBAr^F_4$ were varied, the ratio of acid to catalyst was varied, and the rate at which acid was delivered to the system was varied (e.g., initial full loadings, batch-wise additions, reloadings, or continuous slow additions). None of these studies led to substantial improvement in N_2RR; in all cases, < 2.5 equiv of NH_3 was obtained per $P_3^BFe^+$. Attempts to vary the ratio of the electrode surface area to the working compartment solution volume, either by employing smaller cell geometries or by using different morphologies of glassy carbon as the working electrode (e.g., reticulated porous materials of different pore density or plates of different dimensions), also failed to provide substantial improvement in NH_3 yield. The replacement of $HBAr^F_4$, the original acid used in our electrolysis studies,[6d] by 50 equiv of $[Ph_2NH_2][OTf]$ led to similar yields of NH_3 (Table 5.2, entry 1).

We next investigated the effect of $Cp^*_2Co^+$ as an additive on the electrolysis/electrocatalysis. Traces of relevant cyclic voltammograms (Figure 5.4A and 5.4B) collected with glassy carbon as the working electrode in Et_2O under glovebox atmosphere N_2 at −35 °C are provided. Background traces including only $[Ph_2NH_2][OTf]$ are present in both panels (gray traces). $Cp^*_2Co^+$ (panel A, yellow trace), $Cp^*_2Co^+$ with the addition of ten equiv of $[Ph_2NH_2][OTf]$ (panel A, green trace), $P_3^BFe^+$ (panel B, dark blue trace), $P_3^BFe^+$ with the addition of ten equiv of $[Ph_2NH_2][OTf]$ (panel B, light blue trace), and $P_3^BFe^+$ with the addition of one equiv of $Cp*_2Co^+$ and ten equiv of $[Ph_2NH_2][OTf]$ (both panels, red trace).

Table 5.2. Yields and Faradaic Efficiencies of NH_3 from CPE Experiments with $P_3^BFe^+$

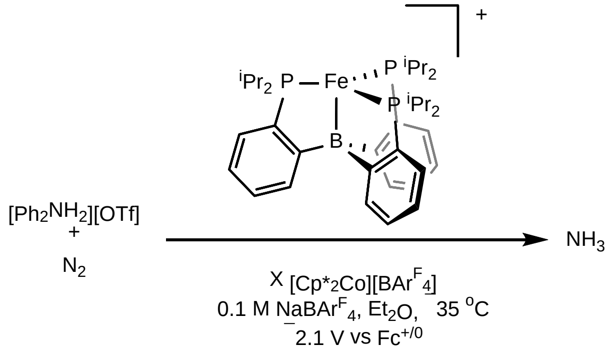

Entry	Equiv $Cp*_2Co^+$	Equiv NH_3 (per Fe)	Equiv NH_3 (per Co)	NH_3 FE (%)
1	0	2.6 ± 0.3[d]	—	24 ± 5
2[a]	0	2.6 ± 0.6	—	18 ± 1
3	1	4.0 ± 0.6	4.0 ± 0.6	28 ± 5
4	5	4.0 ± 0.6[d]	0.8 ± 0.1	25 ± 3
5[a]	5	5.5 ± 0.9[e]	1.1 ± 0.2	19 ± 1
6	10	4 ± 1	0.4 ± 0.1	24 ± 7
7[b]	5	1.9 ± 0.2	0.4 ± 0.1	10 ± 1
8[c]	5	0.9 ± 0.4	0.2 ± 0.1	6 ± 3

All CPE experiments conducted at −2.1 V vs $Fc^{+/0}$ with 0.1 M $NaBAr^F_4$ in Et_2O as solvent at −35 °C under an N_2 atmosphere, featuring a glassy carbon plate working electrode, $Ag^{+/0}$ reference couple isolated by a CoralPor™ frit referenced externally to $Fc^{+/0}$, and a solid sodium auxiliary electrode. Working and auxiliary chambers separated by a sintered glass frit. See SI for further experimental details, controls, and additional data. Averages represent two runs unless noted. [a]After initial electrolysis with 50 equiv $[Ph_2NH_2][OTf]$, an additional 50 equiv $[Ph_2NH_2][OTf]$ in 0.1 M $NaBAr^F_4$ Et_2O solution was added to the working chamber, via syringe through a rubber septum, followed by additional CPE at −2.1 V vs $Fc^{+/0}$. The listed Equiv NH_3 (per Fe) for these runs is the total yield after both electrolysis experiments are completed. ^{b}[$^{2,6\text{-}Cl}PhNH_3$][OTf] employed as the acid. ^{c}[$PhNH_3$][OTf] employed as the acid. ^{d}Average of three runs. ^{e}Average of five runs.

The cyclic voltammogram of $Cp^*_2Co^+$ is shown in panel **A** (yellow trace), displaying the reversible $Cp^*_2Co^{+/0}$ couple at −2.0 V. The addition of [Ph_2NH_2][OTf] to $Cp^*_2Co^+$ causes an increase in current at this potential, consistent with HER

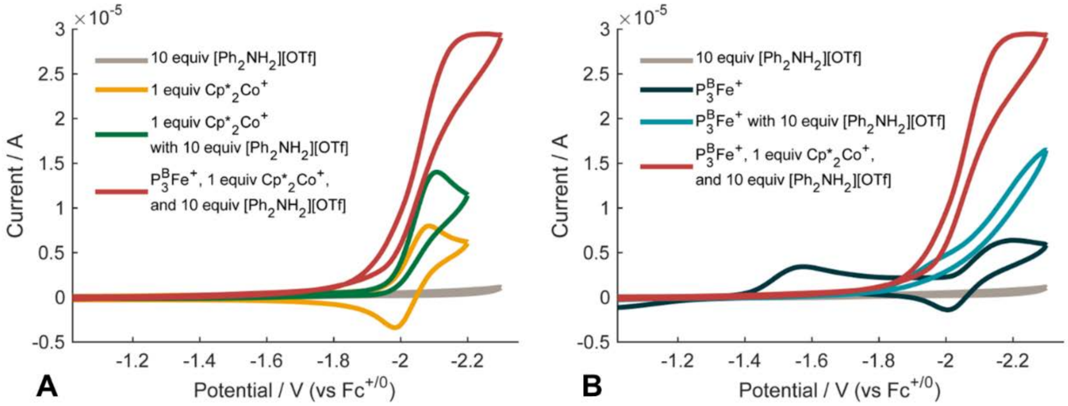

Figure 5.4. A) Cyclic voltammograms of 10 equiv [Ph_2NH_2][OTf] (gray trace), 1 equiv [Cp^*_2Co][BAr^F_4] ($Cp^*_2Co^+$) (yellow trace), 1 equiv $Cp^*_2Co^+$ with 10 equiv [Ph_2NH_2][OTf] (green trace), and $P_3^BFe^+$ with 1 equiv of $Cp^*_2Co^+$ and 10 equiv [Ph_2NH_2][OTf] (red trace). **B**) Cyclic voltammograms of 10 equiv [Ph_2NH_2][OTf] (gray trace), $P_3^BFe^+$ (dark blue trace), $P_3^BFe^+$ with 10 equiv [Ph_2NH_2][OTf] (light blue trace), and $P_3^BFe^+$ with 1 equiv of $Cp^*_2Co^+$ and 10 equiv [Ph_2NH_2][OTf] (red trace). All spectra are collected in 0.1 M $NaBAr^F_4$ solution in Et_2O at −35 °C using a glassy carbon working electrode, and externally referenced to the $Fc^{+/0}$ couple. Scan rate is 100 mV/s.

catalyzed by $Cp^*_2Co^+$ (panel **A**, green trace).

Panel B provides the cyclic voltammogram of $P_3^BFe^+$ in the absence (dark blue trace, showing previously assigned and quasi-reversible $P_3^BFeN_2^{0/-}$ couple at ~ −2.1 V) and in the presence (light blue trace) of $[Ph_2NH_2][OTf]$.[31] The latter is indicative of modest HER and N_2RR. Also evident upon the addition of acid is the disappearance of a wave corresponding to the $P_3^BFe^{+/0}$ couple at ~ −1.6 V. This wave, in the absence of acid, is broad and shows a large peak-to-peak separation, likely due to the presence of both $P_3^BFe^+$ and $P_3^BFeN_2^+$ in solution at −35 °C. The addition of a large excess of $[Ph_2NH_2][OTf]$ presumably results in triflate binding (to generate P_3^BFeOTf, thereby attenuating the waves associated with the reduction of $P_3^BFe^+$ and $P_3^BFeN_2^+$). The red trace of Panel A is reproduced in Panel B to illustrate the marked increase in current observed when $Cp^*_2Co^+$ is added.

CPE studies were undertaken to characterize the reduction products associated with the red trace at ~ −2.1 V vs $Fc^{+/0}$. These studies employed a glassy carbon plate electrode, a $Ag^{+/0}$ reference electrode that was isolated by a CoralPor^{TM} frit and referenced externally $Fc^{+/0}$ redox couple, and a solid sodium auxiliary electrode. The latter was used to avoid excessive, non-productive redox cycling between the working and auxiliary chambers.[32] Unless otherwise noted, CPE experiments were performed at −2.1 V versus $Fc^{+/0}$, with 0.1 M $NaBAr^F_4$ as the ether-soluble electrolyte, under a glovebox N_2 atmosphere at −35 °C. The electrolysis was continued until the current had dropped to 1% of the initial current measured, or until 21.5 hours had passed. The Supporting Information provides additional details.

CPE experiments were conducted with the inclusion of 0, 1, 5, and 10 equiv of $Cp^*{}_2Co^+$ with respect to $P_3^BFe^+$, using excess $[Ph_2NH_2][OTf]$ as the acid. In the absence of added $Cp^*{}_2Co^+$, a significant amount of NH_3 was generated (2.6 ± 0.3 equiv per Fe, entry 1), consistent with the previous finding that, in the presence of a strong acid, $P_3^BFe^+$ can electrolytically mediate N_2-to-NH_3 conversion.[6d] Notably, when a CPE experiment that did not include $Cp^*{}_2Co^+$ was reloaded with additional acid after electrolysis and electrolyzed again, the total yield of NH_3 (2.6 ± 0.6 equiv NH_3 per Fe, entry 2) did not improve.

We found that inclusion of 1.0 equiv of $Cp^*{}_2Co^+$ enhanced the NH_3 yield, by a factor of ~ 1.5 (Table 5.2, entry 3) without decreasing the FE. The data provide a total yield, with respect to both Fe and Co, that confirm modest, but still unequivocal, N_2RR electrocatalysis. In single run experiments, the highest NH_3 yield in the absence of $Cp^*{}_2Co^+$ was 2.8 equiv, compared with 4.4 equiv in the presence of 1 equiv of $Cp^*{}_2Co^+$. Conversely, the lowest single run NH_3 yield in the absence of $Cp^*{}_2Co^+$ was 2.3 equiv, compared with 3.5 equiv in the presence of 1 equiv of $Cp^*{}_2Co^+$.

Increasing the amount of added $Cp^*{}_2Co^+$ did not affect the NH_3 yield (entry 4). However, the addition of a second loading of $[Ph_2NH_2][OTf]$ following the first electrolysis (entry 5), followed by additional electrolysis, led to an improved yield of NH_3, suggesting that some active catalyst is still present after the first run.[6d,9] Even higher $Cp^*{}_2Co^+$ loading did not lead to higher NH_3 yields (entry 6).

CPE of $P_3^BFe^+$ in the presence of $Cp^*{}_2Co^+$ was also explored with other acids. Replacing $[Ph_2NH_2][OTf]$ in these experiments with $[^{2,6\text{-}Cl}PhNH_3][OTf]$ led to lower yields of NH_3, and with $[PhNH_3][OTf]$ even lower yields of NH_3 were observed (entries 7 and 8 respectively). The lower, but nonzero, yield of NH_3 provided by $[PhNH_3][OTf]$ in these

CPE experiments is consistent with chemical trials employing various acids (vide supra) and can be rationalized by the relative pK_a of the acids (Table 5.1). The intermediate yield of NH_3 provided by $[^{2,6\text{-}Cl}PhNH_3][OTf]$ in these CPE experiments is less consistent with simple pK_a considerations, suggesting that additional factors are at play, perhaps including the relative stability of the acid or conjugate base to electrolysis.

To probe whether electrode-immobilized iron might contribute to the N_2RR electrocatalysis, X-ray photoelectron spectroscopy (XPS) was used to study the electrode. After a standard CPE experiment with $P_3^BFe^+$, 5 equiv of $Cp^*{}_2Co^+$, and 50 equiv $[Ph_2NH_2][OTf]$, the electrode was removed, washed with fresh 0.1 M $NaBAr^F{}_4$ Et_2O solution, then fresh Et_2O, and probed by XPS. A *very low* coverage of Fe (< 0.3 atom % Fe) was detected in the post-electrolysis material; no Fe was detected on a segment of the electrode which was not exposed to the electrolytic solution. This observation implies a detectable but likely small degree of degradation of $P_3^BFe^+$ over the course of a 15 hour CPE experiment. Worth noting is that no Co was detected on the post-electrolysis electrode. This may be consistent with the known stability of metallocenes and the recently discovered stability of protonated-Cp* ligands on Rh.[33]

To test whether the small amount of deposited Fe material might be catalytically active for N_2RR, following a standard CPE experiment the electrode was removed from the cold electrolysis solution, washed with fresh 0.1 M $NaBAr^F{}_4$ Et_2O at −35 °C (the electrode itself was maintained at −35 °C at all times), and then used for an additional CPE experiment, under identical conditions except that $P_3^BFe^+$ was excluded. This CPE experiment yielded no detectable NH_3. The charge passed, and H_2 yield, were very similar to a “no $P_3^BFe^+$” control experiment conducted with a freshly cleaned electrode (See SI for further details). Accordingly, a CPE experiment in the absence of $P_3^BFe^+$ demonstrated that $Cp^*_2Co^+$ serves as an effective electrocatalyst for HER with $[Ph_2NH_2][OTf]$ as the acid source, but does not catalyze the N_2RR reaction (0% FE for NH_3, 75% FE for H_2; see SI). This background HER, and the observed catalytic response to the addition of $[Ph_2NH_2][OTf]$ at the $Cp^*_2Co^{+/0}$ couple, provides circumstantial evidence for the formation of a protonated decamethylcobaltocene intermediate, $Cp^*(\eta^4\text{-}C_5Me_5H)Co^+$, on a timescale similar to that of the N_2RR mediated by $P_3^BFe^+$.

To probe whether the sodium auxiliary electrode used in the CPE experiments might play a non-innocent role as a chemical reductant, a standard CPE experiment with $P_3^BFe^+$, 5 equiv $Cp^*_2Co^+$, and 50 equiv $[Ph_2NH_2][OTf]$ was assembled, but was left to stir at −35 °C for 43 hours without an applied potential bias. This experiment yielded 0.3 equiv NH_3 (relative to Fe), suggesting that background N_2RR due to the sodium auxiliary electrode is very minor.

To ensure the NH_3 produced was derived from the N_2 atmosphere during these electrolysis experiments, as opposed to degradation of the anilinium acid used, a standard CPE experiment using $P_3^BFe^+$, 5 equiv $Cp^*_2Co^+$, and 50 equiv of $[Ph_2{}^{15}NH_2][OTf]$ was performed. Only $^{14}NH_3$ product was detected.

We also sought to compare the chemical N_2RR catalysis efficiency of the $P_3^BFe^+$ catalyst under conditions similar to those used for electrocatalysis. Hence, chemical catalysis with $P_3^BFe^+$, employing Cp^*_2Co as a reductant and $[Ph_2NH_2][OTf]$ as the acid at −35 °C instead of the more typical temperature of −78 °C, in a 0.1 M $NaBAr^F_4$ Et_2O solution, afforded lower yields of NH_3 (1.8 ± 0.7 equiv of NH_3 per Fe) than the yields observed via electrolysis with $Cp^*_2Co^+$ as an additive. The lower yields of NH_3 in these chemical trials, compared with our previously reported conditions (12.8 ± 0.5 equiv of NH_3 per Fe at −78 °C),[9] may be attributable to increased competitive HER resulting from a more solubilizing medium (0.1 M $NaBAr^F_4$ Et_2O vs pure Et_2O) and a higher temperature (−35 °C vs −78 °C).[9] These results suggest that an electrochemical approach to NH_3 formation can improve performance, based on selectivity for N_2RR, of a molecular catalyst under comparable conditions.

5.3 Conclusion

Herein we described the first systematic pK_a studies on a synthetic nitrogen fixation catalyst and find a strong correlation between pK_a and N_2RR vs HER efficiency. Chemical studies reveal that, on their own, the anilinium triflate acids employed in the catalysis are unable to generate the N–H bonds of early-stage N_2RR intermediates such as $P_3^BFeNNH_2^+$. We propose that the insolubility of these triflate acids prevents the sufficiently rapid proton transfer necessary to capture the critical but unstable first fixed intermediate, P_3^BFeNNH. Under catalytic conditions, we believe that the presence of the metallocene reductant (Cp^*_2Co) is essential, as this species can be protonated in situ to form $Cp^*(\eta^4\text{-}C_5Me_5H)Co^+$, which in turn is effective in N–H bond formation with early intermediates. This leads to the intriguing conclusion that an intermediate of the background HER pathway is redirected for productive N_2RR chemistry during catalysis.

DFT studies illustrate that the pK_a effect on the N_2RR efficiency may be explained by the variation in the kinetics and thermodynamics of Cp^*_2Co protonation by the different acids. Investigation of the reactivity of $Cp^*(exo\text{-}\eta^4\text{-}C_5Me_5H)Co^+$ with the P_3^BFeNNH intermediate revealed that PCET reactivity, either synchronous or asynchronous, is favorable and may proceed with only a small barrier, suggesting that P_3^BFeNNH can be rapidly trapped by Cp*(*exo*-η^4-C_5Me_5H)Co^+. We suspect Cp*(η^4-C_5Me_5H)Co^+ is likely involved in a variety of N–H bond forming reactions during the overall catalysis, including reactions with late-stage nitrogen fixation intermediates.

Despite the fact that $Cp*_2Co^+$ itself catalyzes HER under the conditions employed for electrocatalytic N_2RR, we found that its inclusion in CPE experiments containing $P_3^BFe^+$ and acid under an N_2 atmosphere led to modest improvements in the overall catalytic yield of NH_3. This system represents what is to our knowledge the first unambiguous example of electrocatalytic N_2RR mediated by a soluble, molecular coordination complex.

5.4 REFERENCES

[1] (a) Yandulov, D. V.; Schrock, R. R. *Science* **2003,** *301*, 76. (b) Arashiba, .; Miyake, Y.; Nishibayashi, Y. *Nat. Chem.* **2010,** *3*, 120. (c) Anderson, J. S.; Rittle, J.; Peters, J. C. *Nature* **2013,** *501*, 84. (d) Imayoshi, R.; Tanaka, H.; Matsuo, Y.; Yuki, M.; Nakajima, K.; Yoshizawa, K.; Nishibayashi, Y. *Angew. Chem. Int. Ed.* **2015**, *21*, 8905.

(e) Ung, G.; Peters, J. C. *Angew. Chem. Int. Ed.* **2015**, *54*, 532. (f) Kuriyama, S.; Arashiba, K.; Nakajima, K.; Matsuo, Y.; Tanaka, H.; Ishii, K.; Yoshizawa, K.; Nishibayashi, Y. *Nat. Commun.* **2016,** *7*, 12181. (g) Hill, P. J.; Doyle, L. R.; Crawford, A. D.; Myers, W. K.; Ashley, A. E. *J. Am. Chem. Soc.* **2016**, *138*, 13521. (h) Buscagan, T. M.; Oyala, P. H.; Peters, J. C. *Angew. Chem. Int. Ed.* **2017**, *56*, 6921. (i) Wickramasinghe, L. A.; Ogawa, T.; Schrock, R. R.; Müller, P. *J. Am. Chem. Soc.* **2017,** *139*, 9132. (j) Fajardo Jr., J.; Peters, J. C. *J. Am. Chem. Soc.* **2017**, *139*, 16105.

[2] (a) Shipman, M. A.; Symes, M. D. *Catal. Today* **2017,** *286*, 57. (b) Kyriakou, V.; Garagounis, I.; Vasileiou, E.; Vourros, A.; Stoukides, M. *Catal. Today* **2017,** *286*, 2.

[3] (a) McKone, J. R.; Marinescu, S. C.; Brunschwig, B. S.; Winkler, J. R.; Gray, H. B. *Chem. Sci.* **2014,** *5*, 865. (b) Bullock, R. M.; Appel, A. M.; Helm, M. L. *Chem. Commun.* **2014,** *50*, 3125.

[4] (a) Benson, E. E.; Kubiak, C. P.; Sathrum, A. J.; Smieja, J. M. *Chem. Soc. Rev.* **2009,** *38*, 89. (b) Appel, A. M.; Bercaw, J. E.; Bocarsly, A. B.; Dobbek, H.; DuBois, D. L.; Dupuis, M.; Ferry, J. G.; Fujita, E.; Hille, R.; Kenis, P. J. A.; Kerfeld, C. A.; Morris, R. H.; Peden, C. H. F.; Portis, A. R.; Ragsdale, S. W.; Rauchfuss, T. B.; Reek, J. N. H.; Seefeldt, L. C.; Thauer, R. K.; Waldrop, G. L. *Chem. Rev.* **2013,** *113*, 6621. (c) Francke, R.; Schille, B.; Roemelt, M. *Chem. Rev.* **2018,** *DOI: 10.1021/acs.chemrev.7b00459*.

[5] Zhang, W.; Lai, W.; Cao, R. *Chem. Rev.* **2017,** *117*, 3717.

[6] (a) Pickett, C. J.; Talarmin, J. *Nature* **1985,** *317*, 652. (b) Al-Salih, T. I.; Pickett, C. J. *J. Chem. Soc. Dalton Trans.* **1985**, 1255. (c) Pickett, C. J.; Ryder, K. S.; Talarmin, J. *J. Chem. Soc. Dalton Trans.* **1986**, 1453. (d) Del Castillo, T. J.; Thompson, N. B.; Peters, J. C. *J. Am. Chem. Soc.* **2016,** *138*, 5341.

[7] In this context, a recent report in which the bioelectrosynthesis of ammonia by nitrogenase is coupled to H_2 oxidation is also noteworthy: Milton, R. D.; Cai, R.; Abdellaoui, S.; Leech, D.; De Lacey, A. L.; Pita, M.; Minteer, S. D. *Angew. Chem. Int. Ed.* **2017,** *56*, 2680.

[8] Very recently there was a report of electrolytic NH_3 synthesis by Cp_2TiCl_2. Although rates and Faradaic efficiencies are discussed, no yields of NH_3 are reported: Jeong, E.-Y.; Yoo, C.-Y.; Jung, C. H.; Park, J. H.; Park, Y. C.; Kim, J.-N.; Oh, S.-G.; Woo, Y.; Yoon, H. C. *ACS Sustainable Chem. Eng.* **2017**, *5*, 9662.

[9] Chalkley, M. J.; Del Castillo, T. J.; Matson, B. D.; Roddy, J. P.; Peters, J. C. *ACS Cent. Sci.* **2017,** *3*, 217.

[10] In some cases, the pK_a of a particular anilinium acid was already known in THF in which case this value was used. In cases where the pK_a has not been reported in THF a literature procedure was used to appropriately convert the pK_a from the solvent in which it was measured into a value for THF. See SI for details.

[11] Consistent with this observation is that efforts to use other weak, non-anilinium acids such as benzylammonium triflate (pK_a in THF of 13.2) and collidinium triflate (pK_a in THF of 11.2) also led to no observed NH_3 formation.

[12] These results are also consistent with our previous observation of $[Ph_2NH_2][OTf]$ (pK_a in THF of 3.2) yielding 72 ± 3 % NH_3. See reference 9.

[13] Pham, D. N.; Burgess, B. K. *Biochemistry* **1993,** *32*, 13275.

[14] In some other reports on N_2RR by molecular catalysts, efficiencies for NH_3 have been reported for several acids, but typically these acids span only a small pK_a range, electron yields are inconsistent, and variations are not explained. For a representative example, see Reference 1b.

[15] Anderson, J. S.; Cutsail III, G. E.; Rittle, J.; Connor, B. A.; Gunderson, W. A.; Zhang, L.; Hoffman, B. M.; Peters, J. C. *J. Am. Chem. Soc.* **2015,** *137*, 7803.

[16] Matson, B. D.; Peters, J. C. *ACS Catal.* **2018,** *8*, 1448.

[17] Recent results on a Cr–N_2 species also support the role of PCET in the formation of early-stage N_2 fixation intermediates in the presence of collidinium triflate and a cobaltocene: Kendall, A. J.; Johnson, S. I.; Bullock, R. M.; Mock, M. T. *J. Am. Chem. Soc.* **2018**, *140*, 2528.

[18] Grimme, S.; Antony, J.; Ehrlich, S.; Krieg, H. *J. Chem. Phys.* **2010**, *132*, 154104.

[19] (a) Tao, J.; Perdew, J. P.; Staroverov, V. N.; Scuseria, G. E. *Phys. Rev. Lett.* **2003,** *91*, 146401. (b) Weigend, F.; Ahlrichs, R. *Phys. Chem. Chem. Phys.* **2005,** *7*, 3297.

[20] For the $P_3^BFeN_xH_y$ and related systems, this combination of functional and basis sets is able to reproduce not only crystallographic details, but also experimentally measured singlet-triplet gaps, reduction potentials, and N–H BDFE's, as described in reference 16.

[21] In all cases where the basicity of $P_3^BFeN_xH_y$ intermediates has been evaluated, they are predicted to be readily protonated by the anilinium triflate acids employed (see SI for details).

[22] DFT calculations suggest that almost all of the $P_3^BFeN_xH_y$ intermediates on the N_2RR pathway have N–H bonds stronger than the C–H bond in $Cp^*(exo\text{-}\eta^4\text{-}C_5Me_5H)Co^+$, suggesting that, at least thermodynamically, the formation of these N–H bonds by PCET is favorable. See reference 16.

[23] The reactivity of ring-functionalized Cp* rings has been discussed previously in the context of electrocatalytic HER by 4d and 5d metals, but via a mechanism involving hydride transfer, rather than via PCET. See: (a) Pitman, C. L.; Finster, O. N. L.; Miller, A. J. M. *Chem. Commun.* **2016**, *52*, 9105. (b) Quintana, L. M. A.; Johnson, S. I.; Corona, S. L.; Villatoro, W.; Goddard, W. A.; Takase, M. K.; VanderVelde, D. G.; Winkler, J. R.; Gray, H. B.; Blakemore, J. D. *Proc. Natl. Acad. Sci.* **2016**, *113*, 6409. (c) Peng, Y.; Ramos-Garcés, M. V.; Lionetti, D.; Blakemore, J. D. *Inorg. Chem.* **2017**, *56*, 10824.

[24] Productive N–H bond formation via PCET with models of late-stage N_2 fixation intermediates (i.e., $M\equiv N$ or $M–NH_2$) has been observed previously: (a) Scepaniak, J. J.; Young, J. A.; Bontchev, R. P.; Smith, J. M. *Angew. Chem. Int. Ed.* **2009**, *48*, 3158. (b) Pappas, I.; Chirik, P. J. *J. Am. Chem. Soc.* **2015**, *137*, 3498. (c) MacLeod, K. C.; McWilliams, S. F.; Mercado, B. Q.; Holland, P. L. *Chem. Sci.* **2016**, *7*, 5736. (d) Lindley, B. M.; Bruch, Q. J.; White, P. S.; Hasanayn, F.; Miller, A. J. M. *J. Am. Chem. Soc.* **2017**, *139*, 5305.

[25] Marcus, R. A. *J. Chem. Phys.* **1956**, *24*, 966.

[26] Iordanova, N.; Decornez, H.; Hammes-Schiffer, S. *J. Am. Chem. Soc.* **2001**, *123*, 3723.

[27] We have assumed a PT-ET mechanism in which ET is rate limiting based on significantly lower reorganization energies and barriers for PT compared to ET. See SI for full description.

[28] Koelle, U.; Infelta, P. P.; Graetzel, M. *Inorg. Chem.* **1988,** *27*, 879.

[29] Call, A.; Casadevall, C.; Acuna-Pares, F.; Casitas, A.; Lloret-Fillol, J. *Chem. Sci.* **2017**, *8*, 4739.

[30] Very recently there has been a study of electrocatalytic N_2RR under ambient conditions in ionic liquids with Fe nanoparticles that reports FE's for NH_3 as high as 60%: Zhou, F.; Azofra, L. M.; Ali, M.; Kar, M.; Simonov, A. N.; McDonnell-Worth, C.; Sun, C.; Zhang, X.; MacFarlane, D. R. *Energy Environ. Sci.* **2017**, *10*, 2516.

[31] We believe that the quasi-reversible nature of the electrochemical couple results from a high reorganization energy, but the couple is fully chemically reversible: Moret, M.-E.; Peters, J. C. *Angew. Chem. Int. Ed.* **2011**, *50*, 2063.

[32] Due to the extensive diffusion between the working and auxiliary chambers, production of an oxidation product which can diffuse to the working electrode and be re-reduced at −2.1 V vs $Fc^{+/0}$ leads to excessive, nonproductive redox cycling between chambers over the course of the lengthy CPE experiments. Sodium metal as an electrode material provides a suitable solution to this technical challenge, as the product of its oxidation (Na^+) is stable to the CPE conditions.